



## Catalytic Decomposition of Formaldehyde on Nanometer Manganese Dioxide

Xiujuan Chu & Hua Zhang (Corresponding author)

Tianjin Municipal Key Lab of Fibres Modification and Functional Fibres Institute of Functional Fibres

Tianjin Polytechnic University

Tianjin 300160, China

Tel: 86-22-2452-8453 E-mail: eva@tjpu.edu.cn

*This research was funded by Tianjin nature science Found (No. 07JCYBJC02400).*

### Abstract

In this paper, nanostructure  $\text{MnO}_2$  was synthesized in aqueous solution, without using any templates, catalysts, and organic reagents. The as-prepared nano- $\text{MnO}_2$  was systematically characterized by X-ray diffraction (XRD), and transmission electron microscopy (TEM) Fourier transform infrared (FT-IR) spectroscopy analysis. The catalytic decompositions of HCHO were studied at different conditions using the nano- $\text{MnO}_2$  as catalyst. The resulting nano- $\text{MnO}_2$  particles were found to exhibit remarkable environmental catalytic performance in catalytic decomposition of formaldehyde in aqueous solution.

**Keywords:** Chemical coprecipitation, Nano- $\text{MnO}_2$ , HCHO, Catalytic decomposition

### 1. Introduction

Manganese oxides ( $\text{MnO}_2$ ) are of considerable interest since these materials can be used in adsorption, catalysis, and other applications. Nano- $\text{MnO}_2$  has a great potentially application in environment protection field as a new generation of environmental friendly catalyst. Cai et al. (2006, p.1971-1976) investigated the removal of a cationic dye, methylene blue, from aqueous solutions by adsorption onto manganese dioxide and found that  $\delta$  manganese dioxide had the strongest ability for removal among the materials. Gaseous toluene can be oxidated into  $\text{CO}_2$  by nano- $\text{MnO}_2$  at ambient temperature (Liu. et al. 2005, p.276-283). Formaldehyde (HCHO) is one of the main pollutants in indoor air. The best way to remove HCHO is to turn it into  $\text{CO}_2$  and  $\text{H}_2\text{O}$ . Yoshika et al. (2002, p.5543-5547) have found that manganese oxide could react with HCHO and release carbon dioxide even at room temperature.

$\text{MnO}_2$  with different physical and chemical properties, such as crystallinity, amount of combined water, specific surface areas, and electrochemical performance, can be yielded under different synthesis conditions. Up to now, many routes for the preparation of  $\text{MnO}_2$  have been developed including thermal oxidation of Mn (II) nitrates, chemical coprecipitation route (Cai et al., 2006, 1971-1976), electrolysis of Mn (II) salts, and sol-gel method. The chemical coprecipitation process was simple and the reaction conditions were easy to control, so it has been widely applied.

In the paper, the chemical coprecipitation process was used to prepare nano- $\text{MnO}_2$  powders. The catalytic decomposition of HCHO was also studied using as-prepared  $\text{MnO}_2$  powders as catalyst at different conditions.

### 2. Experiments

#### 2.1. Chemicals

Potassium permanganate was obtained from Tianjin Standard Science And Technology Co., Ltd. (Tianjin, China). Manganic sulfate was purchased from Tianjin Kermel Chemical Reagent Co.,Ltd. Carmellose Sodium was obtained from Tianjin Bodi Chemical Co., Ltd. All other chemicals were of analytical grade and used without further purification.

#### 2.2. Preparation of the $\text{MnO}_2$ samples

A chemical coprecipitation route was used to prepare  $\text{MnO}_2$  catalyst. The detailed process was as follows: Manganic sulfate were dissolved in distilled water, potassium permanganate aqueous solution was added slowly with magnetic stirring at a molar ratio of  $\text{KMnO}_4/\text{MnSO}_4 = 2/3$  at room temperature. The resulting black solution was kept at room temperature in air for 24 h, then filtered and washed with double deionized water for several times to remove any

soluble products. After that, the deposition was dried at 80 °C in air for about 12 h.

### 2.3. Characterization of the as-prepared MnO<sub>2</sub> particles

Structures of the MnO<sub>2</sub> were characterized using X-ray diffraction (XRD). XRD data were collected using a Rigaku D/MAX 2500 diffractometer with Cu K $\alpha$  radiation ( $\lambda=0.15418\text{nm}$ ). The diffractograms were recorded in the range of 10–80°. Transmission electron microscope (TEM; Hitachi 7650, Japan) was used to observe the morphology of the MnO<sub>2</sub>. FT-IR analysis was carried out on a Nicolet 510P FT-IR spectrophotometer.

### 2.4 Decomposition experiments of HCHO

Under atmospheric pressure, MnO<sub>2</sub> particles were placed in 100mL of glass vessels. And 50mL of HCHO solution with different concentration was introduced into the vessels and the vessels were closed with rubber stopper. The concentrations of HCHO were measured every 12 h. Formaldehyde was spectrophotometrically determined by the acetylacetone method at 412 nm, following Chinese Standards GB18580-2001.

## 3. Results and discussions

### 3.1 Characterization of the as-prepared MnO<sub>2</sub> nanoparticles

Fig.1 shows the XRD recorded for the chemical coprecipitation MnO<sub>2</sub> nanostructures. It can be seen from the figure that the peak profile is broad and most of the peaks ( $2\theta = 23.5^\circ, 37.14^\circ, 42.48^\circ, 56.30^\circ$ ) are indexable to  $\gamma\text{-MnO}_2$  phase with a peak ( $2\theta = 66.84^\circ$ ) of  $\delta\text{-MnO}_2$  phase. The broadness of the peaks indicates that the formed compound has predominantly nanophase.

Fig.2 shows the TEM micrograph MnO<sub>2</sub> particles. The results show distinctly that a nanorod structure with diameter about 5-10nm can be fabricated with this method. Here, we can observe the highly agglomerated nanorods of MnO<sub>2</sub> as shown in the inset of Fig.2.

The FT-IR spectra for MnO<sub>2</sub> before and after catalytic decomposition are shown in Fig.3. Broad absorption peaks centered at around  $3421\text{cm}^{-1}$  and  $1635\text{cm}^{-1}$  are caused by the absorbed water molecules and carbon dioxide because the nanocrystalline materials exhibit a high surface-to-volume ratio (Zhang Y.C. et al, 2005, p. 652-657). A peak due to Mn–O vibrations was observed at  $578\text{cm}^{-1}$  in the spectra of MnO<sub>2</sub>. The band at  $1109\text{cm}^{-1}$  is absorption peak of the Mn-OH functional group, and band at  $1400\text{cm}^{-1}$  are associated with the hydration water of MnO<sub>2</sub>. The FT-IR spectra were no obvious difference between before and after catalytic decomposition.

### 3.2 Catalytic decomposition of HCHO using nano-MnO<sub>2</sub> particles

#### 3.2.1 Effect of initial HCHO concentration

Fig.3 and fig.4 represent the experimental results for the decompositions of HCHO at different initial concentrations using 0.5g nano-MnO<sub>2</sub> powers at 30°C. It is clear that the decomposition of HCHO is relatively high in the region of high HCHO concentration, but it is quickly slowed down in the region of low HCHO concentration (fig.3). The amount HCHO decomposed takes a maximum at the initial concentration of  $0.44\text{mg/m}^3$  (fig.4).

#### 3.2.2 Effect of decomposition temperature

Fig.5 represents the effect of temperature on the decomposition of HCHO at an initial concentration of  $40\text{mg/m}^3$  using 0.5g nano-MnO<sub>2</sub> powers, where the temperature was maintained at 30, 45 and 60 °C. The rate of decomposition of HCHO takes a maximum at 45°C and tends to decrease with the increase or decrease in the temperature, indicating that the catalytic decomposition of HCHO should be carried out at an appropriate temperature.

#### 3.2.3 Effect of amount of nano-MnO<sub>2</sub> particles

Fig.6 shows the effect of applied amount of nano-MnO<sub>2</sub> particles on the removal efficiencies of HCHO at an initial concentration of  $44\text{mg/m}^3$  at 30°C. The removal efficiencies measured after 12 h increased with the amount of nano-MnO<sub>2</sub> particles and reached 87.2% (fig.7) using 0.5 g nano-MnO<sub>2</sub> particles.

## 4. Conclusions

In summary, the nanostructure MnO<sub>2</sub> particles have been prepared using chemical coprecipitation route. We investigated the catalytic decompositions of HCHO at different conditions using the nanostructures MnO<sub>2</sub>. IR spectra indicate that structures of the nano-MnO<sub>2</sub> were no obvious difference between before and after catalytic decomposition. The experimental results show that the catalytic decompositions can be influenced by initial concentration of HCHO, catalytic temperature and amount of nano-MnO<sub>2</sub>.

## References

- Cai D M & Ren N Q. (2006). Removal of methylene blue from aqueous solution onto manganese oxide with various crystal structures [J]. *Acta Scientiarum Circumstantiae*, 2006, 26(12), 1971-1976.
- F. Shiraishi et al. (2005). Decomposition of gaseous formaldehyde in a photocatalytic reactor with a parallel array of

light sources: 1. Fundamental experiment for reactor design. *Chemical Engineering Journal*, 114,153–159.

Li L. et al. (2007). Synthesis and shape evolution of novel cuniform-like  $\text{MnO}_2$  in aqueous solution. *Materials Letters*, 61, 1609–1613.

Li Y D, Li C W & Qian Y T, et al. (1997). Preparation of superfine  $\gamma\text{-MnO}_2$  of different shape [J]. *Chinese Journal of Applied Chemistry*, 14(2), 93-95.

Liu R P, Yang Y L & Xia S J, et al. (2005). Surface chemistry of hydrous manganese dioxide characterization and its effectiveness of removing pollutants [J]. *Environmental Chemistry*, 24(3), 338-341.

Liu Yangsheng & Yi Sha. (2005). Study on oxidation of gaseous toluene by  $\text{MnO}_2$  supported on activated carbon filters. *Journal of Basic Science and Engineering*, 13(3), 276-283.

Yoshika Sekin. (2002). Oxidative decomposition of formaldehyde by metal oxides at room temperature. *Atmospheric Environment*, 36, 5543-5547.

Zhang Y.C., Qiao T., Hu. X.Y & Zhou W.D.. (2005). Simple hydrothermal preparation of  $\gamma\text{-MnOOH}$  nanowires and their low-temperature thermal conversion to  $\beta\text{-MnO}_2$  nanowires [J]. *Journal of Crystal Growth*, 280, 652-657.

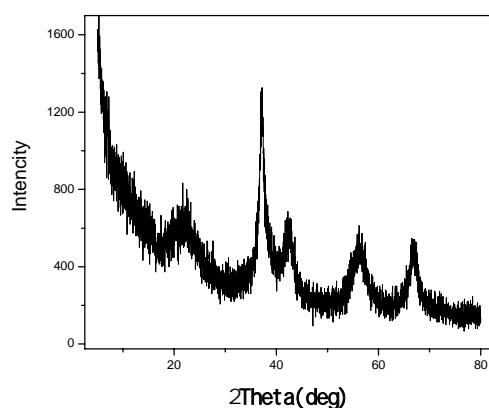


Figure 1. X-ray diffraction patterns of  $\text{MnO}_2$  particles

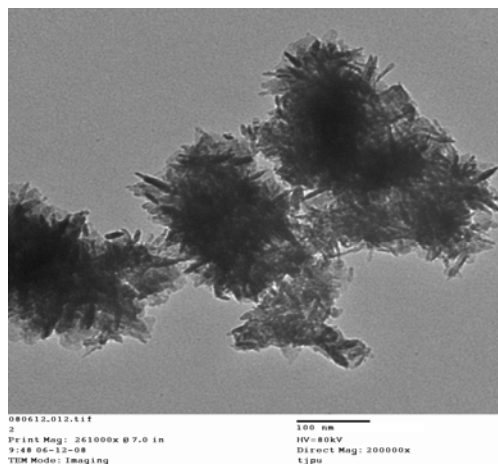


Figure 2. TEM micrograph  $\text{MnO}_2$  particles

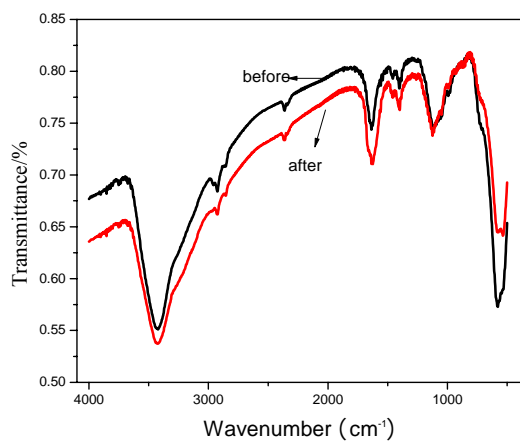


Figure 3. FT-IR spectra for MnO<sub>2</sub>

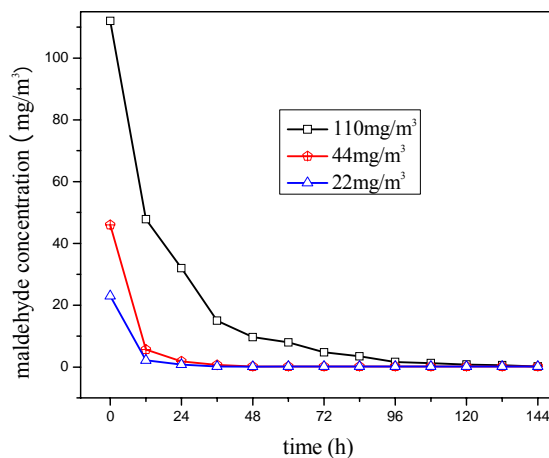


Figure 4. Time courses of concentrations of HCHO at different initial concentration using 0.5g nano-MnO<sub>2</sub> particles at 30°C

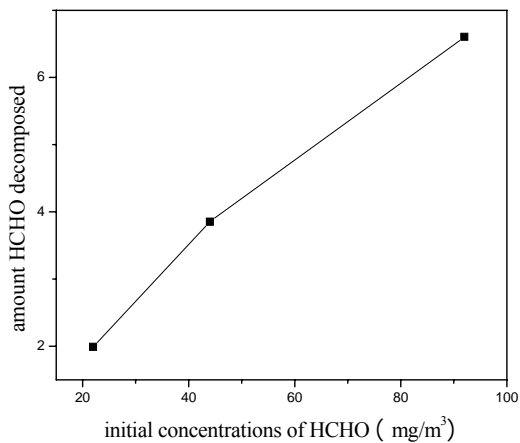


Figure 5. The amount HCHO decomposed at different initial concentration of HCHO using 0.5g nano-MnO<sub>2</sub> particles at 30°C after 12h

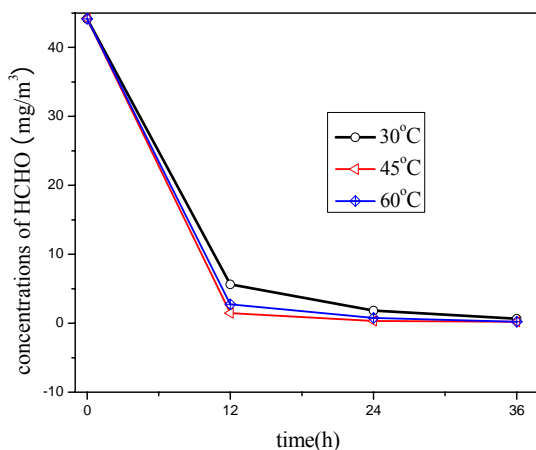


Figure 6. Time courses of concentrations of HCHO at different temperature using 0.5g nano-MnO<sub>2</sub> particles at an initial concentration of 44mg/m<sup>3</sup>

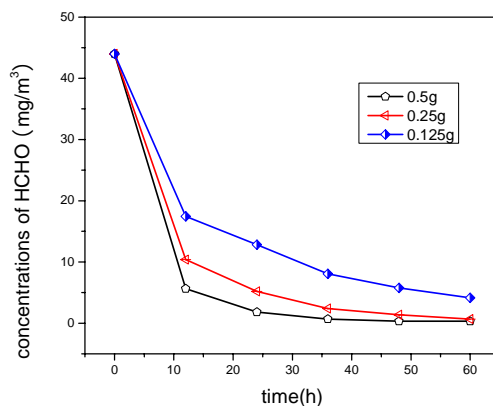


Figure 7. Time courses of concentrations of HCHO at an initial concentration of 44mg/m<sup>3</sup> at 30°C using different amount of nano-MnO<sub>2</sub> particles

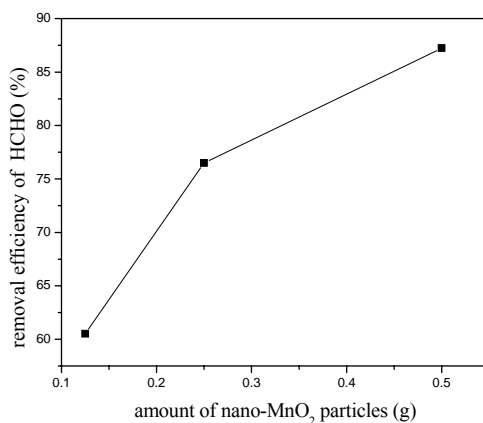


Figure 8. Decomposition rate of HCHO at an initial concentration of 44mg/m<sup>3</sup> at 30°C using different amount of nano-MnO<sub>2</sub> particles after 12h